

COSMOLOGICAL EVOLUTION OF SUPERMASSIVE BLACK HOLES. I. MASS FUNCTION AT $0 < z \lesssim 2$

YAN-RONG LI¹, LUIS C. HO², AND JIAN-MIN WANG^{1,3}

To appear in the Astrophysical Journal

ABSTRACT

We present the mass function of supermassive black holes (SMBHs) over the redshift range $z = 0 - 2$, using the latest deep luminosity and mass functions of field galaxies to constrain the masses of their spheroids, which we relate to SMBH mass through the empirical correlation between SMBH and spheroid mass (the $M_{\bullet} - M_{\text{sph}}$ relation). In addition to luminosity fading of the stellar content of the spheroids, we carefully consider the variation of the bulge-to-total luminosity ratio of the galaxy populations and the $M_{\bullet}/M_{\text{sph}}$ ratio, which, according to numerous recent studies, evolves rapidly with redshift. The SMBH mass functions derived from the galaxy luminosity and mass functions show very good agreement, both in shape and in normalization. The resultant SMBH mass function and integrated mass density for the local epoch ($z \approx 0$) match well those derived independently by other studies. Consistent with other evidence for cosmic downsizing, the upper end of the mass function remains roughly constant since $z \approx 2$, while the space density of lower mass black holes undergoes strong evolution. We carefully assess the impact of various sources of uncertainties on our calculations. A companion paper uses the mass function derived in this work to determine the radiative efficiency of black hole accretion and constraints that can be imposed on the cosmological evolution of black hole spin.

Subject headings: black hole physics – galaxies: evolution – quasars: general

1. INTRODUCTION

Supermassive black holes (SMBHs) are ubiquitous in galaxies with a central stellar bulge (e.g., Magorrian et al. 1998; Ho 1999; Kormendy & Kennicutt 2004), and, via the process of mass accretion (e.g., Salpeter 1964; Zel'dovich & Novikov 1964; Lynden-Bell 1969), power active galactic nuclei (AGNs). The discovery of strong correlations between SMBH mass and the overall properties of the host spheroid, in particular the stellar luminosity, mass, and velocity dispersion (Kormendy & Richstone 1995; Magorrian et al. 1998; Gebhardt et al. 2000; Ferrarese & Merritt 2000; Häring & Rix 2004), has generated intense interest in the notion that black hole and host galaxy growth are closely connected. Studying the mass function of SMBHs and its evolution with redshift is therefore of great significance not only for understanding their cosmological evolution of mass and spin (Shapiro 2005; Wang et al. 2006, 2008, 2009), but also for addressing many issues in galaxy formation (e.g., Di Matteo et al. 2005; Shankar 2009).

Generally speaking, there are two approaches to investigate the SMBH mass function (e.g., Tamura et al. 2006; Shankar 2009). The first approach, which we refer to as theoretically based, stems from the pioneering work of Sołtan (1982). The standard procedure, based on the argument that black hole growth is mainly driven by mass accretion (e.g., Small & Blandford 1992; Marconi et al. 2004; Cao & Li 2008; Shankar et al. 2009b; Cao 2010), is to integrate the continuity equation to determine the number density of SMBHs and to couple it to the AGN luminosity function (LF). Such calculations usually assume two parameters: the radiative efficiency for energy conversion of accretion and the Eddington ratio of

AGNs. As a result, comparing between the predicted SMBH mass function at $z = 0$ with the locally observed quantity sets interesting constraints on the radiative efficiency. The radiative efficiency, averaged over redshift and black hole mass, is found to be $\eta \approx 0.1$ (Yu & Tremaine 2002; Marconi et al. 2004).

The observational approach uses empirical scaling relationships between SMBH mass and host properties, in concert with the LF or stellar mass function (SMF) of the host galaxies, to infer statistical information on the SMBH population (see Shankar 2009 for a review). Most previous works, because of the availability of ample data, have focused on the local ($z \approx 0$) SMBH mass function (e.g., Graham et al. 2007; Vika et al. 2009; Shankar et al. 2009b). Few have treated the evolution of the SMBH mass function. Shankar et al. (2009a) predicted SMBH mass function at $0 < z < 6$ using the local velocity dispersion function of spheroids together with a model for their age distribution; however, their results are highly dependent on the assumed age distribution of the spheroids, which is poorly constrained. Out to intermediate redshifts ($z \approx 1$), Tamura et al. (2006) determined the SMBH mass function by employing a non-evolving relation between SMBH mass and spheroid luminosity ($M_{\bullet} - L_{\text{sph}}$ relation) and by assuming that spheroids evolve passively. A number of recent studies, however, suggest that the black hole-host scaling relations evolve with redshift (McLure et al. 2006; Peng et al. 2006a,b; Ho 2007; Bennert et al. 2010, 2011; Decarli et al. 2010; Merloni et al. 2010). Although the exact magnitude of the effect is not yet well-defined, most studies find that the ratio of black hole mass to spheroid mass is higher in the past. It is essential to take into account these evolutionary effects. At the same time, outstanding progress has been made on deep multiwavelength surveys of normal galaxies and AGNs (e.g., Lawrence et al. 2007; Abazajian et al. 2009). This allows us to construct SMBH mass functions more reliably and to extend them to even higher redshifts than was possible before (e.g., Tamura et al. 2006; Vika et al. 2009, and references therein).

In this work, we aim to derive the SMBH mass function us-

¹ Key Laboratory for Particle Astrophysics, Institute of High Energy Physics, Chinese Academy of Sciences, 19B Yuquan Road, Beijing 100049, China; liyanrong@mail.ihep.ac.cn, wangjm@mail.ihep.ac.cn

² The Observatories of the Carnegie Institution for Science, 813 Santa Barbara Street, Pasadena, CA 91101, USA; lho@obs.carnegiescience.edu

³ National Astronomical Observatories of China, Chinese Academy of Sciences, 20A Datun Road, Beijing 100020, China

ing an up-to-date galaxy LF and SMF, with careful inclusion of various redshift-dependent effects. We extend and update the work of Tamura et al. (2006) out to $z \approx 2$. It is interesting to emphasize that once the SMBH mass function is obtained, a combination of the above two approaches would immediately inform us of the redshift evolution of the radiative efficiency, from which inferences on black hole spins can be made. This is the subject of a companion paper.

This paper is organized as follows. In Section 2, we describe the procedure for deriving the SMBH mass function. Section 3 presents the resultant mass functions and performs a comparison with previous works. We then investigate the uncertainties in our calculations and show how they impact upon the results (Section 4). We discuss the results of this work and the conclusions in Section 5.

2. DERIVATION OF SMBH MASS FUNCTIONS

We employ two methods to derive the SMBH mass function: galaxy LFs, and, alternatively, galaxy SMFs.

We use the recent K -band galaxy LF out to $z \approx 4$ obtained by Cirasuolo et al. (2010), who utilized the first data release of the UKIDSS Ultra Deep Survey. In addition to its depth and large survey area, the Ultra Deep Survey provides reliable photometry in 16 bands. The K band is ideal for this application because it is not severely affected by dust absorption and because it effectively traces the old stellar population and hence is a reliable indicator of stellar mass.

Pérez-González et al. (2008) computed SMF for a sample of $0 < z < 4$ galaxies for which they could obtain rest-frame near-infrared photometry using *Spitzer*/Infrared Array Camera observations. They calculated stellar masses and photometric redshifts by fitting the observational data to ~ 2000 reference templates for which there are reliable spectroscopic redshifts and well-covered spectral energy distributions from the ultraviolet to the mid-infrared bands. The stellar emission models were computed using the code PEGASE (Fioc & Rocca-Volmerange 1997), adopting a Salpeter (1955) initial mass function (IMF) with stellar mass between $0.1 M_\odot$ and $100 M_\odot$.

To derive the SMBH mass function from the galaxy LF or SMF, we need three ingredients: (1) the bulge-to-total luminosity ratio (B/T) to transform the total galaxy luminosity to the spheroid luminosity, for which we assume that the light distribution follows the mass distribution in galaxies; (2) a scaling relation between SMBH mass and the mass of the bulge of the host; and, for the method involving the galaxy LF, (3) a prescription to describe the passive evolution of the spheroid luminosity to account for the evolution of the stellar population. Here we implicitly assume that all the galaxies under consideration possess a bulge component that hosts a black hole (Ho 2008), that the black hole mass scales with the bulge mass, and that the scaling relation evolves with redshift, as described below.

Throughout the paper, we adopt a cosmological model with $\Omega_m = 0.3$, $\Omega_\Lambda = 0.7$, and $H_0 = 70 \text{ km s}^{-1} \text{ Mpc}^{-1}$. Unless otherwise specified, magnitudes are given in the AB system (Oke & Gunn 1983). According to Hewett et al. (2006), for the UKIDSS photometric system, the flux density for the zero point of the Vega-based magnitudes is $f_\nu = 6.31 \times 10^{-21} \text{ erg s}^{-1} \text{ cm}^{-2} \text{ Hz}^{-1}$. The magnitude offset between the Vega-based system and the AB system is $K_{AB} = K_{\text{Vega}} + 1.9$ (Hewett et al. 2006). We adopt a solar K -band luminosity of $L_{\odot,K} = 0.82 \times 10^{32} \text{ erg s}^{-1}$ (see Table 2.1 in Binney & Merrifield

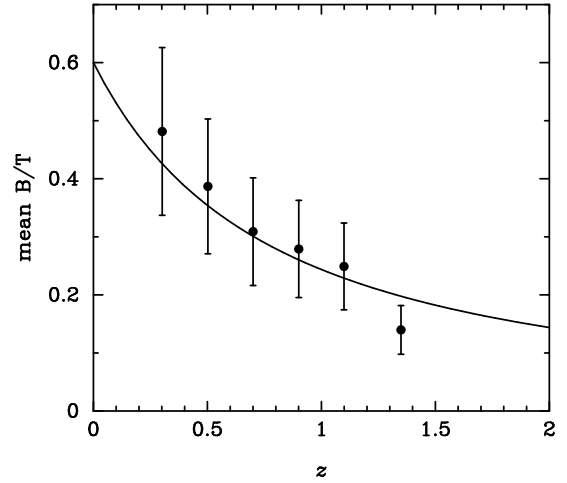


FIG. 1.— Evolution of the bulge-to-total luminosity ratio, B/T. Data points show the mean B/T based on the type-dependent galaxy LFs of Zucca et al. (2006), and the error bars follow from the galaxy LFs. The solid line represents $B/T = 0.6(1+z)^{-1.3}$ (see the text for details).

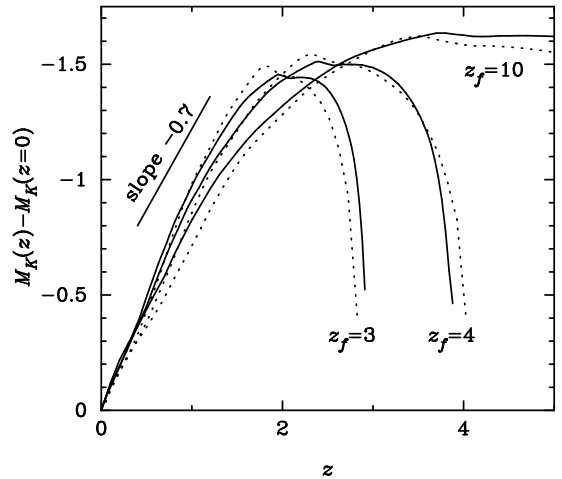


FIG. 2.— Passive evolution of the rest-frame K -band absolute magnitude, calculated using PEGASE (solid lines) and GALAXEV (dotted lines), with formation redshifts $z_f = 3, 4$, and 10 . For $z \lesssim 1.5$ the curves are well approximated by a straight line with a slope of ~ -0.7 .

1998), which corresponds to a solar K -band absolute magnitude of $M_{\odot,K} = 5.2$ in the AB system.

2.1. Bulge-to-total Luminosity Ratio

B/T is an important morphological classification parameter that gives the fraction of the total luminosity contained in the bulge. Observations of local early-type galaxies show that they possess high values of B/T, while late-type galaxies possess lower values of B/T (e.g., Simien & de Vaucouleurs 1986; Schechter & Dressler 1987). Many studies have performed bulge-to-disk decomposition of images of galaxies to quantitatively estimate their B/T (e.g., Kormendy 1977; Kent 1985; Allen et al. 2006; Benson et al. 2007; McGee et al. 2008; Tasca & White 2011). Although its distribution is broad, B/T generally increases with galaxy luminosity (Schechter & Dressler 1987; Benson et al. 2007; Tasca & White 2011). Below we will show how to determine the average value of B/T at $z = 0$, motivated by observations and the comparison between our calculated SMBH mass function and the local observed one.

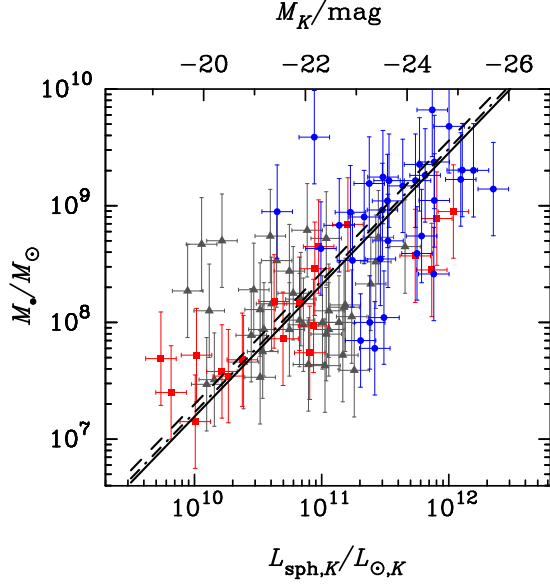


FIG. 3.— $M_{\bullet} - L_{\text{sph}}$ relation in the K band. Lines show the $M_{\bullet} - L_{\text{sph}}$ relation described by Equation (7) at $z = 0$ (solid), $z = 1$ (dashed), and $z = 2$ (dot-dashed). The values of the free parameters are listed in Table 1. Superimposed for comparison are the observational data from Table 3 of Peng et al. (2006b; blue points) and Tables 2 and 3 of Bennert et al. (2010; black triangles and red squares). Note that the tabulated data from Peng et al. (2006b) and Bennert et al. (2010) were not corrected for luminosity evolution; the term accounting for the evolution of the spheroid luminosity in Equation (7) is essential to perform a direct comparison. We adopt k -corrections appropriate for early-type galaxies, assuming $K - V = -2.79$ mag and $K - R = -2.18$ mag (Fukugita et al. 1995; Girardi et al. 2003).

It is difficult to constrain B/T at high redshifts because of the challenges involved in obtaining reliable bulge-to-disk decompositions for distant galaxies. However, we can use the fact that certain characteristic properties of galaxies statistically correlate with B/T to estimate it indirectly at high redshifts. Zucca et al. (2006), using template galaxy spectral energy distributions, classified galaxies out to $z \approx 1.5$ into four spectral types—ranging from early-type to irregulars—and compiled morphological type-dependent galaxy LFs. Their four spectral types roughly correspond to the morphological types E/S0, Sa–Sb, Sc–Sd, and Irr. Based on the average properties of nearby galaxies (e.g., Kent 1985; Weinzirl et al. 2009; Tasca & White 2011), we assign B/T $\approx 0.7, 0.3, 0.1$, and 0.0 , respectively, to the above four type bins. Figure 1 plots the resultant variation of B/T with redshift, where the error bars follow from those of the galaxy LFs. The trend is physically reasonable: the mean B/T decreases systematically and monotonically with increasing redshift. The evolutionary trend can be parameterized as (see also Merloni et al. 2004)

$$\text{B/T} = 0.6(1+z)^{-\gamma}, \quad (1)$$

with $\gamma > 0$, where the normalization is set to B/T = 0.6 at $z = 0$. As shown in Figure 1, $\gamma = 1.3$ gives a reasonably good description of the available data.

This evolutionary trend of B/T can be understood within the framework of hierarchical galaxy formation (e.g., Croton 2006; Khochfar & Silk 2006; Weinzirl et al. 2009), wherein spheroids are built up through two physical processes, mergers and secular evolution. Whereas major mergers scramble disks into (classical) bulges, multiple successive minor mergers can also transform a spiral galaxy into an elliptical (Bournaud et al. 2007). Secular processes from global,

non-axisymmetric structures (e.g., bars and spiral arms) in isolated galaxies further contribute to (pseudo-)bulge growth (Kormendy & Kennicutt 2004, and references therein).

2.2. The $M_{\bullet} - M_{\text{sph}}$ and $M_{\bullet} - L_{\text{sph}}$ Relation

We parameterize the relations between black hole mass and spheroid mass and K -band luminosity as

$$\log \frac{M_{\bullet}}{M_{\odot}} = a_M \log \frac{M_{\text{sph}}}{M_{\odot}} + b_M, \quad (2)$$

and

$$\log \frac{M_{\bullet}}{M_{\odot}} = a_L \log \frac{L_{\text{sph},K}}{L_{\odot,K}} + b_L, \quad (3)$$

where (a_M, b_M, Δ_M) and (a_L, b_L, Δ_L) are parameters to be determined from the data, with Δ_M and Δ_L being the respective intrinsic scatter of each relation. In our calculations, we adopt the $M_{\bullet} - M_{\text{sph}}$ relation derived by Häring & Rix (2004) and the $M_{\bullet} - L_{\text{sph}}$ relation derived by Marconi & Hunt (2003), wherein $(a_M, b_M, \Delta_M) = (1.12 \pm 0.06, -4.12 \pm 0.10, 0.30)$ and $(a_L, b_L, \Delta_L) = (1.13 \pm 0.12, -4.11 \pm 0.07, 0.31)$.

We emphasize that these two correlations pertain solely to nearby galaxies. Redshift-dependent effects should be considered when applying them to higher redshifts. As mentioned above, mounting evidence suggests that the scaling relations between black hole mass and host galaxy evolve with redshift (McLure et al. 2006; Peng et al. 2006a,b; Ho 2007; Bennert et al. 2010, 2011; Decarli et al. 2010; Merloni et al. 2010). Broadly speaking, the ratio of the central SMBH mass and the stellar bulge mass, $M_{\bullet}/M_{\text{sph}}$, tends to be higher at higher redshifts. If we express this redshift dependence as

$$\frac{M_{\bullet}}{M_{\text{sph}}} \propto (1+z)^{\beta}, \quad (4)$$

with $\beta > 0$, the $M_{\bullet} - M_{\text{sph}}$ relation at any given redshift z can be rewritten

$$\log \frac{M_{\bullet}}{M_{\odot}} = a_M \log \frac{M_{\text{sph}}}{M_{\odot}} + b_M + \beta \log(1+z). \quad (5)$$

Similarly, the $M_{\bullet} - L_{\text{sph}}$ relation needs to be modified with the additional term $\beta \log(1+z)$.

Although most recent studies seem to be converging on the idea that black hole growth precedes bulge assembly at higher redshifts, there is no uniform consensus on the exact magnitude of the effect (i.e., the value of β). McLure et al. (2006) estimated the black hole-to-spheroid mass ratio in a sample of radio-loud AGNs, hosted by massive, early-type galaxies in the redshift range $0 < z < 2$, and found that $\beta \approx 2$. Peng et al. (2006b), analyzing the observed R -band $M_{\bullet} - L_{\text{sph}}$ relation for a sample of 31 gravitationally lensed AGNs and 20 unlensed AGNs at $1 \lesssim z \lesssim 4.5$, concluded that, after accounting for luminosity evolution, the $M_{\bullet}/M_{\text{sph}}$ at $z > 1.7$ is ~ 4 times larger than the local value. The implied value of β is ~ 1.4 . In a study of 89 broad-line AGNs between $1 < z < 2.2$ selected from the zCOSMOS survey, Merloni et al. (2010) inferred a somewhat weaker evolution for the ratio of black hole mass to host galaxy stellar mass, with $\beta \approx 0.68$; these authors did not explicitly separate the spheroid mass from the total galaxy mass, and it is possible that $M_{\bullet}/M_{\text{sph}}$ itself may evolve faster than indicated. A relatively strong degree of evolution in $M_{\bullet}/M_{\text{sph}}$, consistent with $\beta \approx 1.3 - 1.4$, was reported by Bennert et al. (2010) for $z \approx 0.4$ and 0.6 , by Decarli et al. (2010) for $0 < z < 3$, and by Bennert et al. (2011) for $1 < z < 2$.

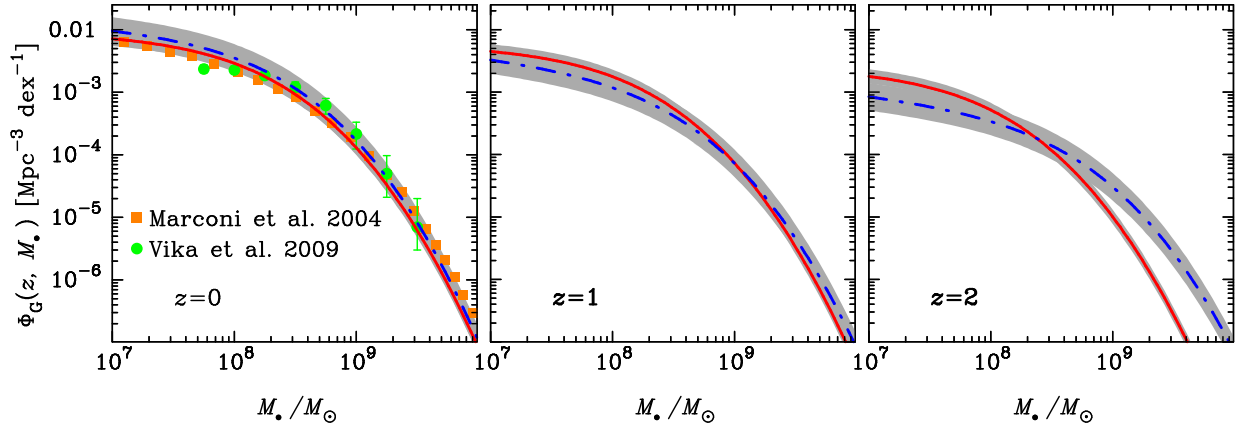


FIG. 4.— SMBH mass function at $z = 0, 1$, and 2 , derived from the galaxy LF (red solid lines) and the galaxy SMF (blue dot-dashed lines). The values of the free parameters are listed in Table 1. Shaded areas represent the errors from the galaxy LF and SMF. In the $z = 0$ panel, the orange squares mark the local SMBH mass function from Marconi et al. (2004), and the green solid points give the corresponding derivation from Vika et al. (2009), whose mass limit is $M_{\bullet} \approx 10^{7.7} M_{\odot}$.

TABLE 1
FREE PARAMETERS

Parameter	Value	Implication
B/T	0.6	Ratio of bulge-to-total luminosity (B/T) at $z = 0$
γ	1.3	Power-law index for the redshift evolution of B/T (Equation 1)
β	1.4	Power-law index for the redshift evolution of $\frac{M_{\bullet}}{M_{\text{sph}}}$ (Equation 4)
Q	0.7	Passive evolution of K -band magnitude (Equation 6)

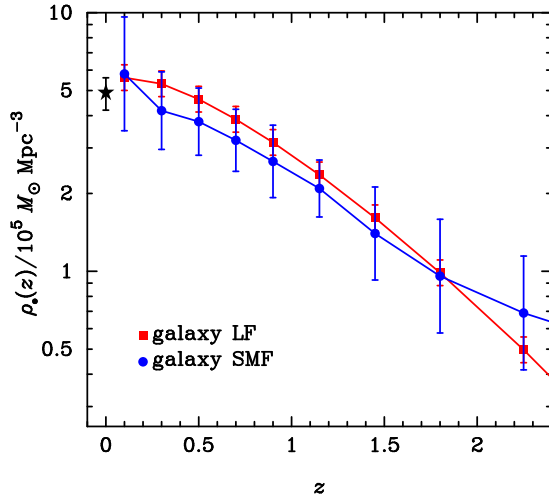


FIG. 5.— SMBH mass density (ρ_{\bullet}) as a function of redshift for $M_{\bullet} > 10^7 M_{\odot}$ derived from the galaxy LF (red squares) and the galaxy SMF (blue points). Redshift bins correspond to the bins chosen by Pérez-González et al. (2008). The black star symbol shows the locally observed value of $\rho_{\bullet} = (4.9 \pm 0.7) \times 10^5 M_{\odot} \text{Mpc}^{-3}$ (Vika et al. 2009).

Based on the above summary, the weight of the current evidence suggests that $M_{\bullet}/M_{\text{sph}}$ evolves with redshift, and, for the parameterization given in Equation (4), that a reasonable choice for the redshift dependence of the evolution is $\beta = 1.4$. We choose this as a fiducial value. Below we will show that the physical requirement that black hole mass density increases monotonically over time places additional constraints on β .

2.3. Passive Evolution of the Spheroid Luminosity

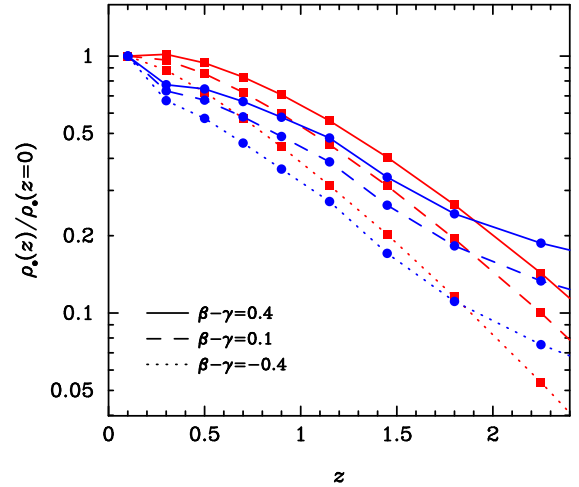


FIG. 6.— SMBH mass density (ρ_{\bullet}) as a function of redshift, normalized to $z = 0$, for $M_{\bullet} > 10^7 M_{\odot}$ and for different combinations of $\beta - \gamma$, derived from the galaxy LF (red squares) and the galaxy SMF (blue points). Redshift bins correspond to the bins chosen by Pérez-González et al. (2008).

When considering the $M_{\bullet} - L_{\text{sph}}$ relation at high redshift—a necessary step for converting the galaxy LF into the SMBH mass function—a correction to the spheroid luminosity must be applied to account for the fading of the stellar population with time. (Note that our alternative procedure of using the galaxy SMF bypasses this complication, and thus serves as a useful consistency check for our LF-based method.) In practice, the correction depends on the star formation history of the spheroid. Following common practice, we employ a single-burst star formation model characterized by an e -folding time τ and a formation redshift z_f . Such a passive evolution scenario traces a single, maximally old stellar pop-

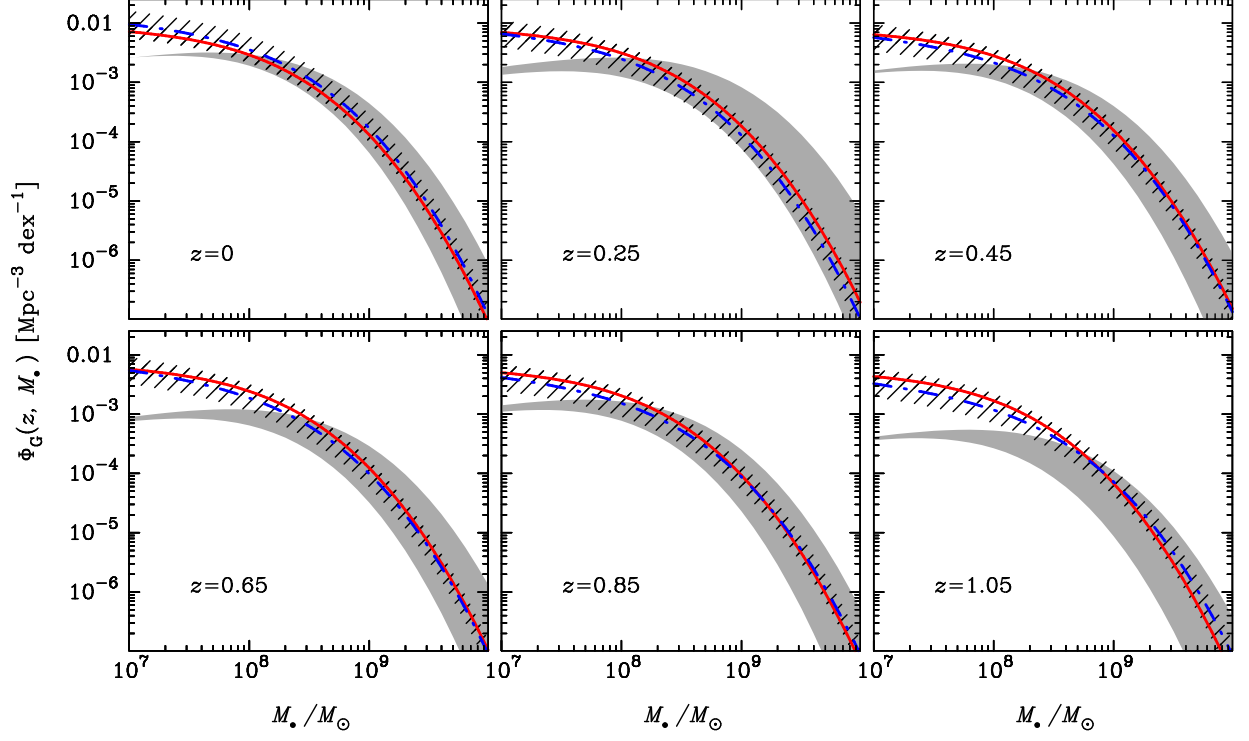


FIG. 7.— Comparison of our SMBH mass function with that derived by Tamura et al. (2006) for different redshift bins. Solid lines and dot-dashed lines are the mass functions derived from the galaxy LF and galaxy SMF, respectively, with hatched areas showing the errors. The shaded area denotes the mass functions derived by Tamura et al. (2006).

ulation and gives a conservative estimate of the amount of luminosity evolution.

We run the code PEGASE (version 2.0; Fioc & Rocca-Volmerange 1997) and GALAXEV (Bruzual & Charlot 2003) to compute the amount of luminosity evolution. Both sets of models use stellar evolutionary tracks from the Padova 1994 library. We assume a Salpeter IMF, a lower mass limit of $0.1 M_\odot$, an upper mass limit of $100 M_\odot$, and solar metallicity. The e -folding time is set nominally to $\tau = 1$ Gyr, and the formation redshift is set to $z_f = 3, 4$, and 10 . The evolution of the rest-frame K -band luminosity is shown in Figure 2. We find that the results are quite insensitive to z_f . For completeness, we also explore models assuming a Chabrier (2003) IMF, as well as metallicities ranging from $0.4 Z_\odot$ to $2.5 Z_\odot$, and $\tau = 0.5 - 2$ Gyr. The results are similar. In all cases, for $z \lesssim 2$, the luminosity evolution in the K band can be described as

$$M_K(z) = M_K(z=0) - Qz, \quad (6)$$

where $Q \approx 0.7$. Including this prescription for luminosity evolution, we can write the $M_\bullet - L_{\text{sph}}$ relation at redshift z as

$$\log \frac{M_\bullet}{M_\odot} = a_L \left(\log \frac{L_{\text{sph}}}{L_\odot} - \frac{Qz}{2.5} \right) + b_L + \beta \log(1+z). \quad (7)$$

Figure 3 plots the $M_\bullet - L_{\text{sph}}$ relation for the set of free parameters tabulated in Table 1. The observed data from Table 3 of Peng et al. (2006b) and Tables 2 and 3 of Bennert et al. (2010) are superimposed for comparison. (Note that the original data were not corrected for luminosity evolution.) This comparison illustrates an important fact: a single $M_\bullet - L_{\text{sph}}$ relation adequately describes the data from $z = 0$ to $z = 2$ after applying our prescriptions for the redshift dependence of $M_\bullet / M_{\text{sph}}$ and spheroid luminosity evolution. This verifies the robustness of our redshift-dependent corrections and reaffirms

the conclusions of previous studies, such as those of Peng et al. (2006a,b), Bennert et al. (2010, 2011), and Decarli et al. (2010).

Having introduced the above three components (for the redshift evolution of B/T, $M_\bullet / M_{\text{sph}}$, and bulge luminosity), we can relate the SMBH mass function to the galaxy LF, accounting for intrinsic scatter in the $M_\bullet - L_{\text{sph}}$ relation:

$$\Phi_G(z, M_\bullet) = 2.5 \frac{d \log L_{\text{sph},K}}{d M_\bullet} \int d \log L_{\text{sph},K} \Phi(z, M_K) \times \frac{1}{\sqrt{2\pi} \Delta_L} \exp \left[-\frac{(\log L_{\text{sph},K} - \log M_\bullet)^2}{2 \Delta_L^2} \right], \quad (8)$$

where M_K is the total K -band absolute magnitude of the galaxy, $L_{\text{sph},K}$ is the luminosity of the bulge, $\Phi(z, M_K)$ is the K -band galaxy LF given by Cirasuolo et al. (2010), and Φ_G measures the mass function per unit volume per unit mass. Here the subscript “G” distinguishes the mass function of galaxies from that of AGNs. The factor $d \log L_{\text{sph},K} / d M_\bullet = 1 / [\ln(10) a_L M_\bullet]$, according to Equation (3). The transformation between $L_{\text{sph},K}$ and M_K reads

$$M_K = M_{\odot,K} - 2.5 \log \left(\frac{1}{B/T} \frac{L_{\text{sph},K}}{L_{\odot,K}} \right). \quad (9)$$

Expressing the galaxy LF as a Schechter (1976) function (Cirasuolo et al. 2010),

$$\Phi(z, M_K) = 0.4 \ln(10) \Phi_0 10^{-0.4(\alpha+1)\Delta M} \exp[-10^{-0.4\Delta M}], \quad (10)$$

with $\Delta M = M_K - M_K^*$,

$$M_K^*(z) = M_K^*(z=0) - \left(\frac{z}{z_M} \right)^{k_M}, \quad (11)$$

and

$$\Phi_0(z) = \Phi_0(z=0) \exp \left[- \left(\frac{z}{z_\phi} \right)^{k_\phi} \right]. \quad (12)$$

The free parameters are $\alpha = -1.07 \pm 0.1$, $z_M = 1.78 \pm 0.15$, $k_M = 0.47 \pm 0.2$, $z_\phi = 1.70 \pm 0.09$, $k_\phi = 1.47 \pm 0.1$, $M_K^*(z=0) = -22.26$ (fixed), and $\Phi_0(z=0) = (3.5 \pm 0.4) \times 10^{-3} \text{ Mpc}^{-3}$ (see Table 1 in Cirasuolo et al.).

Similarly, the SMBH mass function is related to the galaxy SMF as

$$\Phi_G(z, M_\bullet) = \frac{d \log M_{\text{sph}}}{d M_\bullet} \int d \log M_{\text{sph}} \Phi(z, M_{\text{tot}}) \times \frac{1}{\sqrt{2\pi} \Delta_M} \exp \left[- \frac{(\log M_{\text{sph}} - \log M_\bullet)^2}{2 \Delta_M^2} \right], \quad (13)$$

where M_{tot} is the total galaxy stellar mass, $M_{\text{sph}} = M_{\text{tot}}(B/T)$ is the mass contained in the bulge, and $\Phi(z, M_{\text{tot}})$ is the galaxy SMF given by Pérez-González et al. (2008). The factor $d \log M_{\text{sph}} / d M_\bullet = 1 / [\ln(10) a_M M_\bullet]$, according to Equation (2). The galaxy SMF, also expressed as a Schechter function (Pérez-González et al. 2008), is

$$\Phi(z, M) = \ln(10) \Phi_* \left(\frac{M}{M_*} \right)^{1+\alpha} \exp \left(- \frac{M}{M_*} \right). \quad (14)$$

The parameters α , M_* , and Φ_* are given in Table 2 of Pérez-González et al. for 12 redshift bins from $z=0$ to $z=4$.

3. RESULTS

3.1. SMBH Mass Functions

Figure 4 shows the SMBH mass function, computed using the galaxy LF and SMF, at $z=0, 1$, and 2 . The lowest redshift bin of Cirasuolo et al.'s LFs is at $z=0.3$, and we extrapolate it to $z=0$. We confirm that the extrapolation is consistent with the observed local K -band galaxy LF (e.g., Devoreux et al. 2009, and references therein). The SMBH mass functions derived from the galaxy LF and SMF show strikingly good agreement, both in shape and in normalization. A notable discrepancy occurs at $z=2$, where the SMF-based SMBH mass function systematically lies above that derived from the galaxy LF, for $M_\bullet \gtrsim (2-3) \times 10^8 M_\odot$. As this corresponds roughly to the “knee” of the mass function, we expect this result to be quite sensitive to the values of M_* and Φ_* of the SMF. Curiously, inspection of the data in Pérez-González et al. (2008) reveals that M_* and Φ_* show significant fluctuations precisely at the redshift bins $z=1.8$ and $z=2.25$; it is unclear whether the magnitude of these fluctuations is sufficient to account for deviations in the SMF-based SMBH mass function at $z=2$.

For comparison, we superpose the local ($z \approx 0$) SMBH mass functions derived by Marconi et al. (2004) and Vika et al. (2009). The agreement is excellent. We note that the mass function at the high-mass end hardly evolves from $z \approx 2$ to $z=0$, indicating that the most massive black holes have been largely in place since $z \approx 2$ and experience little growth since then (Marconi et al. 2004; McLure & Dunlop 2004). By contrast, the lower end of the mass function undergoes strong evolution. This trend is often referred to as cosmic “downsizing.”

We calculate the mass density for SMBHs for $M_\bullet > 10^7 M_\odot$ by integrating the mass functions and show the results in Figure 5. Once again, the results derived separately

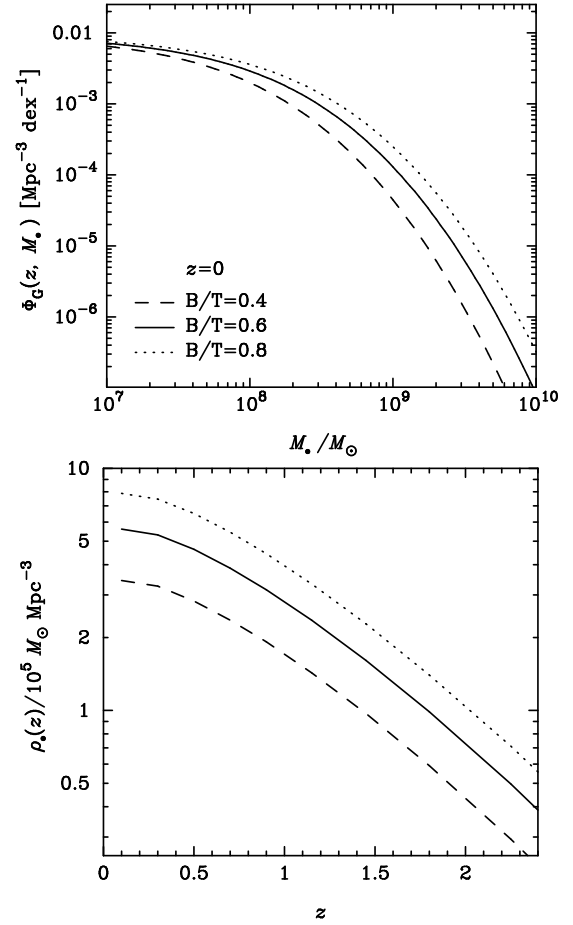


FIG. 8.— SMBH mass function at $z=0$ (top) and mass density as a function of z (bottom) for $B/T = 0.4, 0.6$, and 0.8 .

from the galaxy LF and SMF are quite consistent. The mass density increases rapidly from $z=2$ until $z \approx 0.5$, below which it begins to saturate, converging toward the local ($z \approx 0$) mass density of $\rho_\bullet = (4.9 \pm 0.7) \times 10^5 M_\odot \text{ Mpc}^{-3}$ derived by Vika et al. (2009; black star). In light of the accretion paradigm for AGN activity and black hole growth, this is in line with the redshift evolution of AGN activity, which reaches a maximum around $z \approx 2-3$ (e.g., Ueda et al. 2003; Hopkins et al. 2007) and rapidly declines toward lower redshifts, such that by the present-day universe most black holes are highly sub-Eddington and nearly quiescent (Ho 2008, 2009).

3.2. Constraints on the Free Parameters

Table 1 lists the values of the free parameters we used to describe the redshift evolution of B/T , $M_\bullet / M_{\text{sph}}$, and luminosity of the stellar population. Their impact on the SMBH mass function can be inferred from Equations (7) and (9). In the Appendix, we explicitly show how these parameters affect the SMBH mass density.

The preceding section explains how we adopt the values of key free parameters in our calculations, motivated by various lines of observations. Using the galaxy LFs for four bins of morphological types from Zucca et al. (2006), we obtain $\gamma = 1.3$ for the power-law redshift dependence of B/T and a normalization factor of $B/T \approx 0.6$ at $z=0$. It is interesting to point out that an average B/T of 0.6 yields a black hole mass function in good agreement with the local observational data, as shown in Figure 4. Furthermore, that the SMBH mass

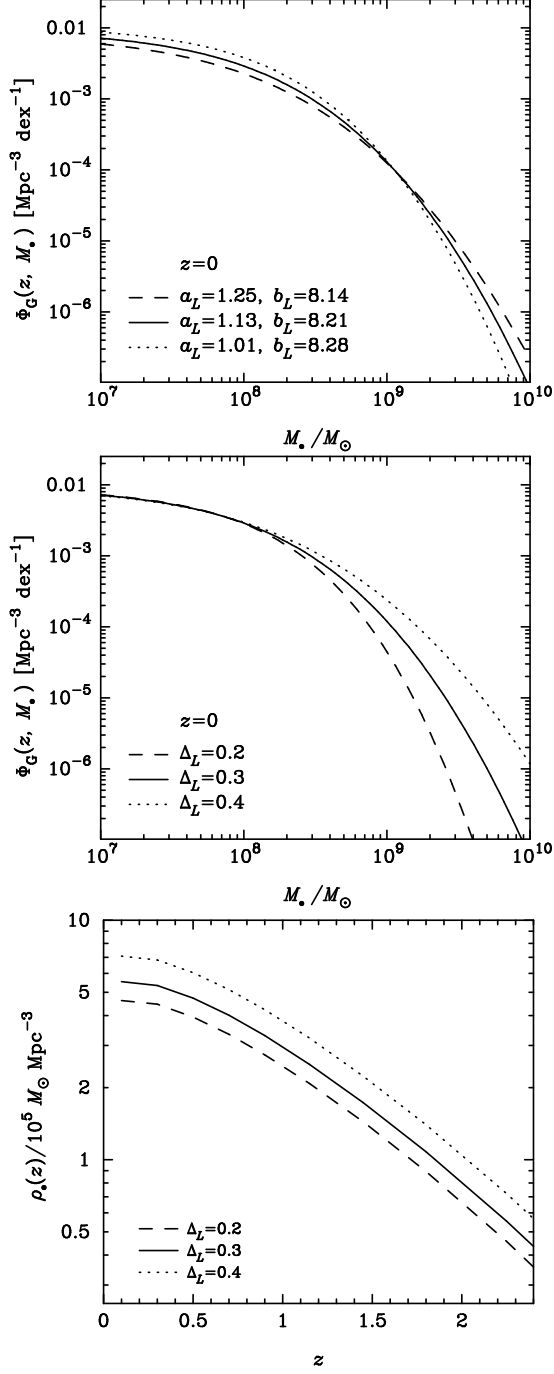


FIG. 9.— Effect on our calculations from the uncertainties from the $M_\bullet - L_{\text{sph}}$ relation given by Marconi & Hunt (2003). (Top) SMBH mass functions at $z=0$ for different values of the fitting errors for the $M_\bullet - L_{\text{sph}}$ relation. (Middle) SMBH mass functions at $z=0$ for three values of the intrinsic scatter Δ_L for the $M_\bullet - L_{\text{sph}}$ relation. (Bottom) SMBH mass densities corresponding to the three mass functions of the middle panel.

function derived from the galaxy LF matches well those obtained from the SMF testifies to the robustness of the spheroid luminosity evolution correction adopted in our calculations. Here we additionally show that the physical condition that the SMBH mass density always necessarily increases over cosmic time imposes additional constraints on the evolution of the $M_\bullet / M_{\text{sph}}$ ratio. In the Appendix, we prove that the SMBH

mass density derived from the galaxy LF is proportional to

$$\rho_\bullet(z) \propto (1+z)^{\beta-\gamma a_L} 10^{(z/z_M)^{k_M} / 2.5 - a_L Qz / 2.5} \Phi_0(z), \quad (15)$$

where a_L is the slope of the $M_\bullet - L_{\text{sph}}$ relation (see Equation (3)) and z_M, k_M , and $\Phi_0(z)$ are the parameters of the Cirasuolo et al. (2010) galaxy LF (see Equations (11) and (12)). We note that the parameters γ and β are degenerate along lines of constant $\beta - \gamma a_L$. Since $a_L \approx 1$, for the purposes of this discussion let us set $a_L = 1$ for convenience. For a fixed γ and a large value of β , the first term in Equation (15) increases monotonically with redshift and dominates over the others; an increase of ρ_\bullet with redshift is physically prohibited. Figure 6 illustrates ρ_\bullet derived for three choices of $\beta - \gamma$. While the case with $\beta - \gamma = -0.4$ yields a rapid drop off of ρ_\bullet around $z=0$, the case with $\beta - \gamma = 0.4$ leads to a negative increase. Both cases seem unlikely and conflict with the basic physical requirement that ρ_\bullet must increase with time and that most black holes are nearly quiescent by the present-day universe. Note that, for ρ_\bullet derived from the galaxy SMF, there is a sharp transition between the redshift bins $z=0.1$ and $z=0.3$; this may be due to the large uncertainties of the SMF at $z=0.1$ (see Pérez-González et al. 2008). Inspection of Figure 6 suggests that, if $\gamma \approx 1.3$, a reasonable value of β should be $\lesssim 1.7$. Future observations will empirically test this assertion.

3.3. Comparison with Previous Results

In Figure 7, we perform a comparison of our results with those of Tamura et al. (2006). We find good agreement for the massive end of the mass functions, for $M_\bullet \gtrsim 10^{8.3} M_\odot$, but the Tamura et al. results systematically fall below ours toward lower masses. We ascribe these discrepancies to three factors.

(1) The survey depths of the galaxy LFs are very different. Tamura et al. employ the galaxy LFs from the COMBO-17 survey (Bell et al. 2004), whose depth in the B band is ~ 25 mag (Vega), which corresponds to $K \approx 21$ mag (Vega). By comparison, the Cirasuolo et al. LFs reach $K \approx 23$ mag (Vega; Lawrence et al. 2007), allowing us to reach significantly further down the mass function, robustly sampling later type galaxies and lower mass black holes.

(2) Tamura et al. only consider early-type galaxies, which occupy the luminous end of the galaxy LF and host exclusively massive black holes. We, on the other hand, have sufficient sensitivity to sample later type galaxies, which have proportionately lower mass bulges and hence black holes. Thus, it is not a surprise that our results agree with those of Tamura et al. at the high-mass end of the mass function but diverge toward lower masses. The excellent match between our results and those independently obtained by Marconi et al. (2004) and Vika et al. (2009) at $z \approx 0$ (Figure 4) testifies to the robustness of our assumptions.

(3) Our calculations take into account the redshift-dependent evolution of B/T and $M_\bullet / M_{\text{sph}}$, while Tamura et al. adopt constant values for these parameters. However, for a given total galaxy luminosity and our chosen prescription for passive evolution of the spheroid light,⁴ B/T and $M_\bullet / M_{\text{sph}}$ have opposite effects on the black hole masses. In other words, the parameters γ and β , which describe the evolution of B/T and $M_\bullet / M_{\text{sph}}$, respectively, are degenerate. Because we use $\gamma = 1.3$ and $\beta = 1.4$, in practice these two components nearly cancel each other out in terms of their effects

⁴ Like us, Tamura et al. (2006) also compute passive evolution using the PEGASE code.

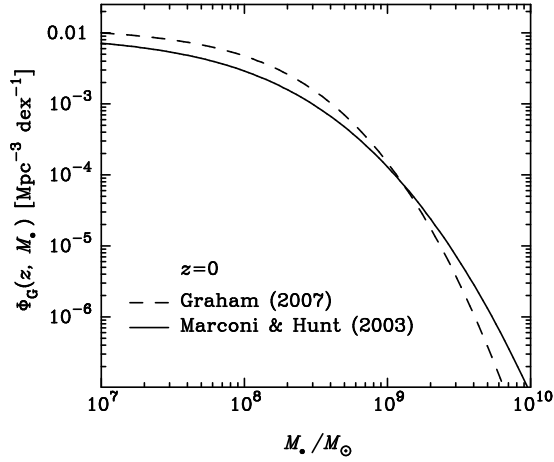


FIG. 10.— SMBH mass function at $z = 0$ for the $M_{\bullet} - L_{\text{sph}}$ relation from Marconi & Hunt (2003; solid line), which is assumed in our calculations, and for that from Graham (2007; dashed line), who reanalyzed the data of Marconi & Hunt.

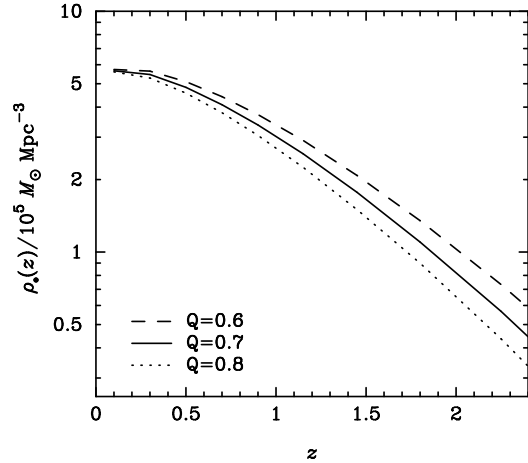


FIG. 11.— SMBH mass density for three choices of the passive evolution parameter, $Q = 0.6, 0.7$, and 0.8 .

on black hole masses at high redshift (see Equations (7) and (9)). Therefore, inclusion of the redshift-dependent evolution of B/T and $M_{\bullet}/M_{\text{sph}}$, in fact, induces only mild differences.

4. SOURCES OF UNCERTAINTIES

As the galaxy LF and SMF are well described by a Schechter function, the exponential decline beyond the knee implies that even minor changes in the high-luminosity or high-mass end can induce significant effects on the upper end of the SMBH function. Here we examine the impact of various sources of uncertainties on our derivation of the SMBH mass function. For simplicity, we report only on results based on the galaxy LF; the results based on the galaxy SMF are similar.

4.1. Bulge-to-total Luminosity Ratio

Figure 8 shows SMBH mass functions and mass densities for B/T = 0.4, 0.6, and 0.8 at $z = 0$. As to be expected because of the exponential drop off of the galaxy LF, the high-mass end of the black hole mass function is especially sensitive to the value of B/T. For a given total galaxy luminosity, larger B/T leads to larger black hole masses and hence to a larger number density and integrated mass density of SMBHs. The

parameter γ , which measures the redshift evolution of B/T, is degenerate with respect to β . Therefore, we treat $\beta - \gamma a_L$ as one independent parameter and have shown its influence on the SMBH mass density in Section 3.2 and in Figure 6.

In our calculations, for the sake of simplicity, we neglect the dependence of B/T on the galaxy luminosity or mass, and just focus on its average dependence on redshift. Schechter & Dressler (1987) show that the bulge-to-disk ratio varies weakly with galaxy luminosity, roughly as $(L/L_{\star})^{0.28}$ (see also Figure 12 of Benson et al. 2007). For $L \approx 0.1L_{\star}$ to $10L_{\star}$, B/T increases from ~ 0.45 to 0.75 , if we normalize B/T to 0.6 for $L = L_{\star}$. This luminosity-dependent variation of B/T is small, and we neglect it. We further neglect any intrinsic dispersion in the average value of B/T at a given morphological type, as this dispersion is poorly quantified even for nearby galaxies (e.g., Simien & de Vaucouleurs 1986; de Jong 1996).

4.2. The Local $M_{\bullet} - L_{\text{sph}}$ Relation

The upper panel of Figure 9 shows the fitting errors of the $M_{\bullet} - L_{\text{sph}}$ relation derived by Marconi & Hunt (2003) and their corresponding influences on our results. We find that the reported uncertainties on the slope and normalization (a_L and b_L) of the $M_{\bullet} - L_{\text{sph}}$ relation induce only minor effects on the overall SMBH mass function. Marconi & Hunt (2003) reported an intrinsic scatter of $\Delta_L \approx 0.3$ for the $M_{\bullet} - L_{\text{sph}}$ relation. To assess its impact on our results, we calculate the mass function and mass density for three values of Δ_L (0.2, 0.3, and 0.4), as shown in the middle and bottom panels of Figure 9. We find that Δ_L has a remarkably large impact on the shape of the upper end of the mass function. This is again due to the exponential decline of the galaxy LF. However, the effect of Δ_L on the mass density is relatively insignificant, changing the overall amplitude by $\sim \pm 25\%$.

Graham (2007) reanalyzed the work of Marconi & Hunt (2003), updating some of the data on black hole masses and galaxy magnitudes. He reports a somewhat shallower $M_{\bullet} - L_{\text{sph}}$ relation, with best-fit parameters $(a_L, b_L, \Delta_L) = (0.93, -1.80, 0.33)$. Figure 10 compares the effect that the two versions of the $M_{\bullet} - L_{\text{sph}}$ relation have on our derived SMBH mass function, assuming an intrinsic scatter of $\Delta_L = 0.3$. The differences are minor over all masses.

Two caveats should be kept in mind. First, recent studies suggest that classical bulges and pseudo-bulges may obey somewhat different scaling relations with black hole mass (e.g., Greene et al. 2008; Jiang et al. 2011; Kormendy et al. 2011; Xiao et al. 2011). Another complication arises from the possibility that, at a given redshift, galaxies in different evolutionary phases may have different values of $M_{\bullet}/M_{\text{sph}}$ (e.g., Alexander et al. 2008; Lamastra et al. 2010). Unfortunately, the current data on the bulge properties of high-redshift galaxies are far too crude to allow us to concretely address either of these issues.

4.3. Choice of Passive Evolution

We assume that the stellar population of the bulge formed in a single burst at a formation redshift of $z_f = 3, 4$, and 10 , thereafter fading passively as $M_K(z) = M_K(z = 0) - Qz$, with $Q \approx 0.7$. As we can see from Figure 2, the value of Q is quite insensitive to z_f . In Figure 11, we examine the sensitivity of the SMBH mass density to the value of Q , choosing values of $0.6, 0.7$, and 0.8 . Variations of this magnitude on Q have only a mild influence on ρ_{\bullet} .

4.4. Summary of the Uncertainties

Among the uncertainties discussed above, the most important are those related with the local $M_\bullet - L_{\text{sph}}$ relation. While uncertainties in the slope and zero point of the relation affect the SMBH mass function at the level of $\lesssim 0.2$ dex over the entire mass range, the upper end of the mass function is especially sensitive to the intrinsic scatter of the $M_\bullet - L_{\text{sph}}$ relation. Changing the scatter at the level of ± 0.1 dex affects the mass function by $\sim \pm 0.5$ dex at $M_\bullet \approx 2 \times 10^9 M_\odot$. This is due to the exponential falloff of the galaxy LF, such that even a minor change in luminosity leads to a significant variation in the galaxy number density, and hence in the SMBH number density. In a similar manner, the upper end of the SMBH mass function is sensitive to the values of B/T. In our calculations, the redshift evolution of B/T, encapsulated in the parameter γ , is degenerate with the evolution of M_\bullet/M_{sph} , which is parameterized by β . Fortunately, for reasonable choices of γ and β , which are well motivated by current observations, the redshift evolution of B/T and M_\bullet/M_{sph} largely cancel out. Plausible variations on the prescription for passive evolution of the spheroid luminosity also introduce relatively minor perturbations on our results. In summary, from inspection of the tests presented in Figures 6 and 8–11, it seems that the total uncertainties on the SMBH mass function are generally within ~ 0.3 dex.

Lastly, it is worth emphasizing that the stellar masses used to compute the galaxy SMF of Pérez-González et al. (2008) assume a Salpeter IMF. As has been pointed out by a number of authors (e.g., Bell et al. 2003; Bruzual & Charlot 2003; Pozzetti et al. 2007), the Salpeter IMF is too rich in low-mass stars and might overestimate the stellar masses. The Chabrier (2003) IMF may yield more reasonable stellar masses (e.g., di Serego Alighieri et al. 2005). Stellar masses derived with the Chabrier IMF are smaller than those derived with the Salpeter IMF by a factor of ~ 1.7 (e.g., Pozzetti et al. 2007). Consequently, the characteristic mass M_\star of the Pérez-González et al. galaxy SMF would be lower by this amount. In the power-law regime ($M \lesssim M_\star$), this is equivalent to a decrease of Φ_\star by a factor of $\sim (1.7)^{1+\alpha}$ (see Equation (14)). For a characteristic value of $\alpha \approx -1.2$ (Pérez-González et al. 2008), Φ_\star , and thus the magnitude of SMBH mass function, decreases slightly by ~ 0.05 dex in the power-law regime. Beyond the knee ($M > M_\star$), however, the exponential decline of

the SMF significantly affects the magnitude of SMBH mass function. Nevertheless, the resultant SMBH mass density decreases systematically only by a factor of ~ 1.7 (0.23 dex).

However, the existing observations of the local SMBH mass function and mass density (e.g., Marconi et al. 2004; Vika et al. 2009) place constraints on the adopted IMF parameters. If the Chabrier IMF is adopted, a mismatch will be induced between the SMBH mass function and the existing observations, and other parameters in the calculations will have to be modified accordingly (e.g., increasing B/T). Note that if the Chabrier IMF is universal and invariant with redshift, it will not affect the overall evolution of the SMBH mass function, and the present results remain unchanged.

5. SUMMARY

We derive the SMBH mass function from $z = 0$ to $z = 2$ using the up-to-date, deep, wide-area K -band galaxy LF of Cirasuolo et al. (2010), and, in a complementary manner, using the galaxy SMF of Pérez-González et al. (2008). In addition to extending much further down the mass function than previous studies, enabling us to robustly sample later type galaxies and lower mass black holes, our analysis carefully considers redshift-dependent corrections to the average B/T of the galaxy populations, the M_\bullet/M_{sph} ratio, and the stellar luminosity of the bulge. We find excellent agreement between the SMBH mass functions derived from the galaxy LFs and the galaxy SMFs. Moreover, the resultant SMBH mass function and integrated mass density for the local epoch match well those derived independently by other studies.

In a companion paper, we will use the SMBH mass function obtained in this work to determine the radiative efficiency of black hole accretion as a function of redshift, with the goal of constraining the cosmological evolution of black hole spin.

Y.R.L. thanks N. Tamura for providing the data of their SMBH mass function, and F. Shankar and X.-W. Cao for useful discussions. We thank the referee for helpful suggestions, and members of the IHEP AGN group for discussions. This research is supported by NSFC-10733010, -10821061 and -11173023, and 973 project (2009CB824800). The work of LCH is supported by the Carnegie Institution for Science.

APPENDIX

REDSHIFT DEPENDENCE OF SMBH MASS DENSITY

In this appendix, we clarify how the SMBH mass density depends on certain free parameters adopted in our analysis. The Schechter (1976) function used to describe the galaxy LF has the general form

$$\Phi(z, L) dL = \Phi_0(z) \left(\frac{L}{L_\star} \right)^{-\alpha} \exp \left(-\frac{L}{L_\star} \right) \frac{dL}{L_\star}, \quad (\text{A1})$$

where $\Phi_0(z)$ is the normalization and L_\star is the characteristic luminosity as a function of redshift. If, for the sake of simplicity, we neglect the intrinsic scatter of the $M_\bullet - L_{\text{sph}}$ relation in Equation (3), the SMBH mass function $\Phi_G(z, M_\bullet)$ is related to the galaxy LF as

$$\Phi_G(z, M_\bullet) dM_\bullet = \Phi(z, L) dL. \quad (\text{A2})$$

Integrating the SMBH mass function, we obtain the total black hole mass density

$$\rho_\bullet(z) = \int \Phi_G(z, M_\bullet) M_\bullet dM_\bullet \propto \int \Phi(z, L) M_\bullet dL. \quad (\text{A3})$$

According to the $M_\bullet - L_{\text{sph}}$ relation (Equation 7), the black hole mass can be expressed as

$$M_\bullet = 10^{b_L - a_L Qz/2.5} (1+z)^\beta [(B/T)L]^{a_L}. \quad (\text{A4})$$

Hence,

$$\rho_{\bullet}(z) = 10^{b_L - a_L Qz/2.5} (1+z)^{\beta} \Phi_0(z) L_{\star}(z) (B/T)^{a_L} \Gamma(1 - \alpha + a_L), \quad (\text{A5})$$

where a_L is the slope of the $M_{\bullet} - L_{\text{sph}}$ relation (see Equation (3)), $\Phi_0(z)$ is given by Equation (12), and $\Gamma(x)$ is the Gamma function. Since the characteristic luminosity from Equation (11) is

$$L_{\star}(z) = L_{\star}(z=0) 10^{(z/z_M)^{k_M}/2.5}, \quad (\text{A6})$$

we have

$$\rho_{\bullet}(z) \propto (1+z)^{\beta - \gamma a_L} 10^{(z/z_M)^{k_M}/2.5 - a_L Qz/2.5} \Phi_0(z). \quad (\text{A7})$$

We note that, apart from being sensitive to the details of the galaxy LF, the redshift evolution of the SMBH mass density depends on the chosen prescription for the redshift evolution of B/T , the $M_{\bullet} - L_{\text{sph}}$ relation, and luminosity variation of the stellar population. The parameters γ and β are degenerate along lines of constant $\beta - \gamma a_L$. The physical requirement that ρ_{\bullet} always increases with time places additional constraints on the redshift dependence of these parameters (see also Hopkins et al. 2006).

REFERENCES

- Abazajian, K. N., Adelman-McCarthy, J. K., Ag eros, M. A., et al. 2009, *ApJS*, 182, 543
- Alexander, D. M., Brandt, W. N., Smail, I., et al. 2008, *AJ*, 135, 1968
- Allen, P. D., Driver, S. P., Graham, A. W., et al. 2006, *MNRAS*, 371, 2
- Bell, E. F., McIntosh, D. H., Katz, N., & Weinberg, M. D. 2003, *ApJS*, 149, 289
- Bell, E. F., Wolf, C., Meisenheimer, K., et al. 2004, *ApJ*, 608, 752
- Bennert, V. N., Auger, M. W., Treu, T., Woo, J.-H., & Malkan, M. A. 2011, *arXiv:1102.1975*
- Bennert, V. N., Treu, T., Woo, J., et al. 2010, *ApJ*, 708, 1507
- Benson, A. J., D zanovi , D., Frenk, C. S., & Sharples, R. 2007, *MNRAS*, 379, 841
- Binney, J., & Merrifield, M. 1998, *Galactic Astronomy* (Princeton, NJ: Princeton Univ. Press)
- Bournaud, F., Jog, C. J., & Combes, F. 2007, *A&A*, 476, 1179
- Bruzual, G., & Charlot, S. 2003, *MNRAS*, 344, 1000
- Cao, X. 2010, *ApJ*, 725, 388
- Cao, X., & Li, F. 2008, *MNRAS*, 390, 561
- Chabrier, G. 2003, *PASP*, 115, 763
- Cirasuolo, M., McLure, R. J., Dunlop, J. S., et al. 2010, *MNRAS*, 401, 1166
- Croton, D. J. 2006, *MNRAS*, 369, 1808
- Decarli, R., Falomo, R., Treves, A., et al. 2010, *MNRAS*, 402, 2453
- de Jong, R. S. 1996, *A&A*, 313, 45
- Devereux, N., Willner, S. P., Ashby, M. L. N., Willmer, C. N. A., & Hriljac, P. 2009, *ApJ*, 702, 955
- Di Matteo, T., Springel, V., & Hernquist, L. 2005, *Nature*, 433, 604
- di Serego Alighieri, S., Vernet, J., Cimatti, A., et al. 2005, *A&A*, 442, 125
- Ferrarese, L., & Merritt, D. 2000, *ApJ*, 539, L9
- Fioc, M., & Rocca-Volmerange, B. 1997, *A&A*, 326, 950
- Fukugita, M., Shimasaku, K., & Ichikawa, T. 1995, *PASP*, 107, 945
- Gebhardt, K., Bender, R., Bower, G., et al. 2000, *ApJ*, 539, L13
- Girardi, M., Mardirossian, F., Marinoni, C., Mezzetti, M., & Rigoni, E. 2003, *A&A*, 410, 461
- Graham, A. W. 2007, *MNRAS*, 379, 711
- Graham, A. W., Driver, S. P., Allen, P. D., & Liske, J. 2007, *MNRAS*, 378, 198
- Greene, J. E., Ho, L. C., & Barth, A. J. 2008, *ApJ*, 688, 159
- H ring, N., & Rix, H.-W. 2004, *ApJ*, 604, L89
- Hewett, P. C., Warren, S. J., Leggett, S. K., & Hodgkin, S. L. 2006, *MNRAS*, 367, 454
- Ho, L. C. 1999, in *Observational Evidence for Black Holes in the Universe*, ed. S. K. Chakrabarti (Dordrecht: Kluwer), 157
- Ho, L. C. 2007, *ApJ*, 669, 821
- Ho, L. C. 2008, *ARA&A*, 46, 475
- Ho, L. C. 2009, *ApJ*, 699, 626
- Hopkins, P. F., Richards, G. T., & Hernquist, L. 2007, *ApJ*, 654, 731
- Hopkins, P. F., Robertson, B., Krause, E., Hernquist, L., & Cox, T. J. 2006, *ApJ*, 652, 107
- Jiang, Y.-F., Greene, J. E., & Ho, L. C. 2011, *ApJ*, 737, L45
- Kent, S. M. 1985, *ApJS*, 59, 115
- Khochfar, S., & Silk, J. 2006, *MNRAS*, 370, 902
- Kormendy, J. 1977, *ApJ*, 217, 406
- Kormendy, J. 2004, in *Carnegie Observatories Astrophysics Series, Vol. 1: Coevolution of Black Holes and Galaxies*, ed. L. C. Ho (Cambridge: Cambridge Univ. Press), 1
- Kormendy, J., Bender, R., & Cornell, M. E. 2011, *Nature*, 469, 374
- Kormendy, J., & Kennicutt, R. C. 2004, *ARA&A*, 42, 603
- Kormendy, J., & Richstone, D. 1995, *ARA&A*, 33, 581
- Lamastra, A., Menci, N., Maiolino, R., Fiore, F., & Merloni, A. 2010, *MNRAS*, 405, 29
- Lawrence, A., Warren, S. J., Almaini, O., et al. 2007, *MNRAS*, 379, 1599
- Lynden-Bell, D. 1969, *Nature*, 223, 690
- Magorrian, J., Tremaine, S., Richstone, D., et al. 1998, *AJ*, 115, 2285
- Marconi, A., & Hunt, L. K. 2003, *ApJ*, 589, L21
- Marconi, A., Risaliti, G., Gilli, R., et al. 2004, *MNRAS*, 351, 169
- McGee, S. L., Balogh, M. L., Henderson, R. D. E., et al. 2008, *MNRAS*, 387, 1605
- McLure, R. J., & Dunlop, J. S. 2004, *MNRAS*, 352, 1390
- McLure, R. J., Jarvis, M. J., Targett, T. A., Dunlop, J. S., & Best, P. N. 2006, *MNRAS*, 368, 139
- Merloni, A., Bongiorno, A., Bolzonella, M., et al. 2010, *ApJ*, 708, 137
- Merloni, A., Rudnick, G., & Di Matteo, T. 2004, *MNRAS*, 354, L37
- Oke, J. B., & Gunn, J. E. 1983, *ApJ*, 266, 713
- Peng, C. Y., Impey, C. D., Ho, L. C., Barton, E. J., & Rix, H.-W. 2006a, *ApJ*, 640, 114
- Peng, C. Y., Impey, C. D., Rix, H.-W., et al. 2006b, *ApJ*, 649, 616
- P rez-Gonz lez, P. G., Rieke, G. H., Villar, V., et al. 2008, *ApJ*, 675, 234
- Pozzetti, L., Bolzonella, M., Lamareille, F., et al. 2007, *A&A*, 474, 443
- Salpeter, E. E. 1955, *ApJ*, 121, 161
- Salpeter, E. E. 1964, *ApJ*, 140, 796
- Schechter, P. 1976, *ApJ*, 203, 297
- Schechter, P. L., & Dressler, A. 1987, *AJ*, 94, 563
- Shankar, F. 2009, *New Astron. Rev.*, 53, 57
- Shankar, F., Bernardi, M., & Haiman, Z. 2009a, *ApJ*, 694, 867
- Shankar, F., Weinberg, D. H., & Miralda-Escud , J. 2009b, *ApJ*, 690, 20
- Shapiro, S. L. 2005, *ApJ*, 620, 59
- Simien, F., & de Vaucouleurs, G. 1986, *ApJ*, 302, 564
- Small, T. A., & Blandford, R. D. 1992, *MNRAS*, 259, 725
- Sothan, A. 1982, *MNRAS*, 200, 115
- Tamura, N., Ohta, K., & Ueda, Y. 2006, *MNRAS*, 365, 134
- Tasca, L. A. M., & White, S. D. M. 2011, *A&A*, 530, A106
- Ueda, Y., Akiyama, M., Ohta, K., & Miyaji, T. 2003, *ApJ*, 598, 886
- Vika, M., Driver, S. P., Graham, A. W., & Liske, J. 2009, *MNRAS*, 400, 1451
- Wang, J.-M., Chen, Y.-M., Yan, C.-S., & Hu, C. 2008, *ApJ*, 673, L9
- Wang, J.-M., Chen, Y.-M., & Zhang, F. 2006, *ApJ*, 647, L17
- Wang, J.-M., Hu, C., Li, Y.-R., et al. 2009, *ApJ*, 697, L141
- Weinzirl, T., Jogee, S., Khochfar, S., Burkert, A., & Kormendy, J. 2009, *ApJ*, 696, 411
- Xiao, T., Barth, A. J., Greene, J. E., et al. 2011, *ApJ*, in press
- Yu, Q., & Tremaine, S. 2002, *MNRAS*, 335, 965
- Zel'dovich, Y. B., & Novikov, I. D. 1964, *Dokl. Akad. Nauk SSSR*, 158, 811
- Zucca, E., Ilbert, O., Bardelli, S., et al. 2006, *A&A*, 455, 879